

Scientific Paper

Doi: <http://dx.doi.org/10.1590/1809-4430-Eng.Agric.v43n1e20220109/2023>

## ORBITAL REMOTE SENSING FOR THE MANAGEMENT OF AREAS IRRIGATED WITH A CENTRAL PIVOT SYSTEM

Wendel K. O. Moreira<sup>1\*</sup>, Marcio F. Maggi<sup>1</sup>, Luan P. Venancio<sup>2</sup>,  
Claudio L. Bazzi<sup>3</sup>, Igor S. Santos<sup>2</sup>

<sup>1\*</sup>Corresponding author. Universidade Estadual do Oeste do Paraná/Cascavel - PR, Brasil.

E-mail: [wendelmoreira21@outlook.com](mailto:wendelmoreira21@outlook.com) | ORCID ID: <http://orcid.org/0000-0002-7778-0151>

### KEYWORDS

irrigation  
management,  
irrigation  
management zones,  
cotton,  
evapotranspiration.

### ABSTRACT

Irrigated agriculture is considered one of the most important techniques for agricultural production in the world, despite being the sector that uses water resources the most. Thus, technological advances have been constantly developed and applied in the sector as a way to improve water management and reduce its consumption, considering that some cultures are affected by economic costs and feasibilities of production, because the water cost has increased significantly in recent years. Remote sensing is a technology that has provided good results for estimating evapotranspiration (ET<sub>r</sub>) in producing areas, enabling more efficient irrigation management for low costs. This study aimed to answer the question about how the generation of irrigation management zones (IMZs) can be used to optimize water use and improve irrigation systems and which ET<sub>r</sub> models are better for it. Three ET<sub>r</sub> estimation models (Surface Energy Balance Algorithm for Land [SEBAL], Mapping Evapotranspiration at High Resolution and with Internalized Calibration [METRIC] and Simple Algorithm for Evapotranspiration Retrieving [SAFER]) were used to design IMZs in center pivot cultivated with cotton. The design of IMZs with ET<sub>r</sub> data proved to be a viable alternative, making it possible to improve water management in irrigated systems, reducing costs with viability irrigation for cotton and others cultures. The METRIC method displayed the greatest ease in obtaining the data used in the ET<sub>r</sub> estimation for generating the IMZs.

### INTRODUCTION

Irrigated agriculture is considered one of the most important techniques for world agricultural production, despite being the sector that uses the most water resources. However, the improvement of irrigation infrastructure can reduce the amount of water used by up to 50% of the collected water (Barkhordari & Hashemy Shahdany, 2022). As the cost of water resources has increased, mainly due to reduced availability, as well as the need to increase production efficiency, greater interest has been given to managing variable rate irrigation (VRI) and the use of various technologies (Sharma & Irmak, 2021).

This fact has been noticed with the almost daily appearance of terms such as “Precision Agriculture (PA),” “intelligent agriculture,” “Internet of Things (IoT),” “Internet of everything (IoE),” “computing in cloud,” “cloud computing,” “big data,” “data analysis,” and “machine learning,” among others, aiming to apply computational resources focused on agricultural practices (Morais et al., 2019), which aim at developing tools capable of assisting professionals and rural producers in the management of agricultural production systems with agility and precision, seeking to optimize the agricultural production systems and the natural resources.

<sup>1</sup> Universidade Estadual do Oeste do Paraná (UNIOESTE)/Cascavel - PR, Brasil.

<sup>2</sup> Universidade Federal de Viçosa (UFV)/Viçosa - MG, Brasil.

<sup>3</sup> Universidade Tecnológica Federal do Paraná (UTFPR)/Medianeira - PR, Brasil.

Area Editor: Fernando França da Cunha

Received in: 2-11-2022

Accepted in: 10-18-2022

PA has, in its structure, a subarea called precision irrigation (PI) or VRI, which aims to optimize the use of water resources in irrigation, considering the spatiotemporal application of water to maximize production and minimize environmental impacts, allowing a reduction of up to 50% in the amount of water to be used (Neupane & Guo, 2019).

VRI has become technically feasible; however, crop water status mapping is necessary to combine irrigation amounts with site-specific crop water demands (Gobbo et al., 2019), although deciding when and where water should be applied has proven problematic (Chastain et al., 2016). An alternative that has been evolving for decades is remote sensing (RS), which can provide maps with sufficient details in a timely manner (Peschechera et al., 2019; Ahmad et al., 2021) and, in some situations, with constant data.

Several applications can be made from RS data, including crop evapotranspiration (ET<sub>r</sub>) estimates, using models and/or specific algorithms such as the *Aerodynamic Resistance-Surface Energy Balance approach* (RSEB) (Kalma & Jupp, 1990), *Surface Energy Balance Index* (SEBI) (Menenti & Choudhury, 1993), *Surface Energy Balance Algorithm for Land* (SEBAL) (Bastiaanssen et al., 1998), *Mapping Evapotranspiration at High Resolution and with Internalized Calibration* (METRIC) (Allen et al., 2007) and *Simple Algorithm for Evapotranspiration Retrieving* (SAFER) (Teixeira, 2010), among others.

These algorithms have been applied for various purposes, such as the management of irrigated crops (Souza et al., 2019; Yang et al., 2022), quantification of watershed evaporation (Chao et al., 2021), and determination of agricultural crop ET<sub>r</sub> (Grosso et al., 2018).

The application of models is an alternative to the design of irrigation management zones (IMZs). This was proven by Gobbo et al. (2019), who applied data generated from the SEBAL model to create IMZs in a pivot-irrigated field in northeastern Italy, which showed promising results for irrigation scheduling. Currently, few studies have evaluated the application of ET<sub>r</sub> data in the design for the construction of IMZs; therefore, the objective of this research was to apply the data from three ET<sub>r</sub> estimation models (METRIC, SEBA, and SAFER) to the design of IMZs as an alternative to optimize water use more effectively in center pivot cultivated with cotton.

## MATERIAL AND METHODS

### Description of the study area

The study was conducted on a commercial farm located in the municipality of São Desidério, in the western region of the state of Bahia, with a mean altitude of 741 m and geographic coordinates of 12° 53' 13.11" S and 45° 30' 44.49" W (Figure 1). According to the climate classification of Köppen (1884), the climate of the region is classified as Aw, tropical with rainy summers and dry winters, with annual rainfall from 1,000–1,300 mm, concentrated between October and April (Alvares et al., 2013). For this study, two of the 12 center pivots available at the site were used to obtain the data (center pivots P7 and P8), which had a useful area of nearly 143 ha and 133 ha, respectively (Figure 1). The data used refers to cotton (FM975 variety) cultivation in 2018, 2019, and 2020.

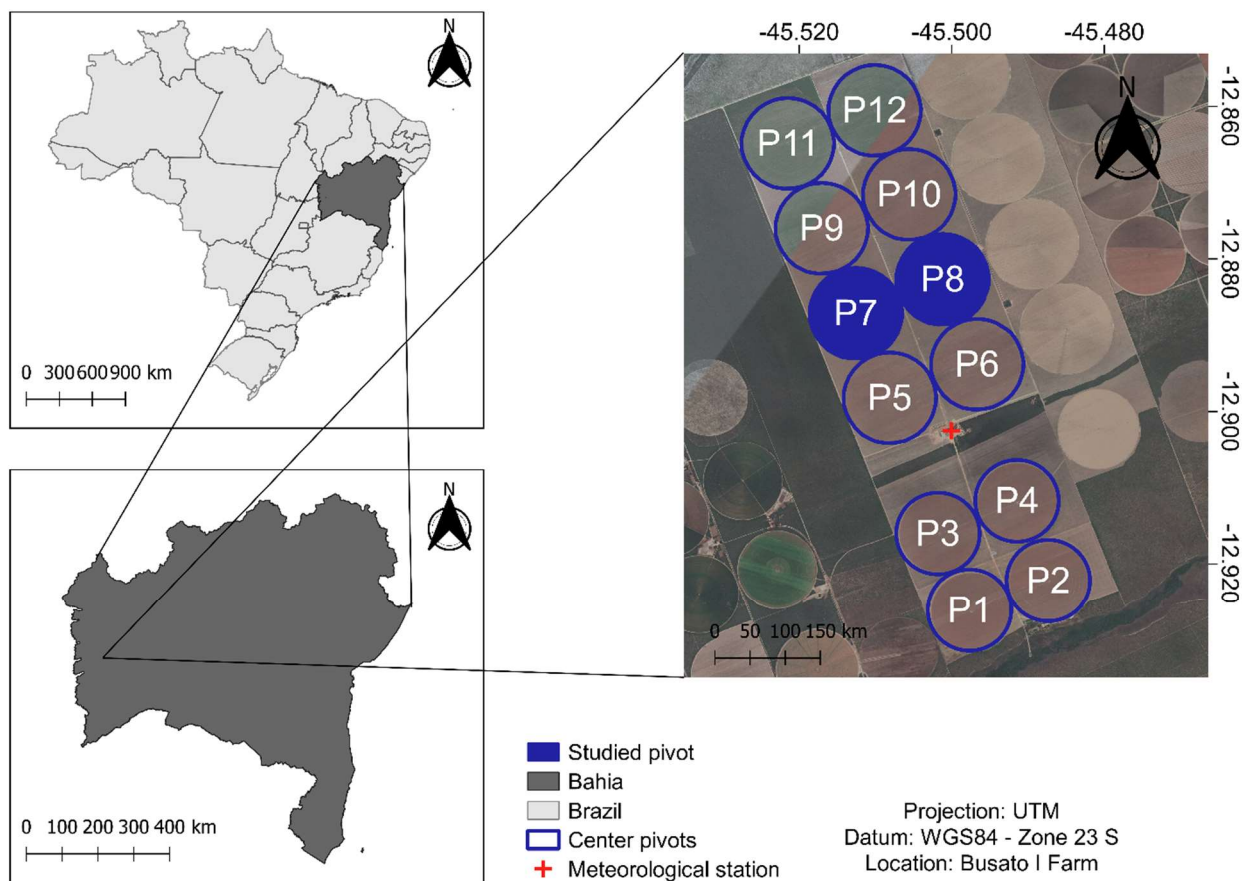


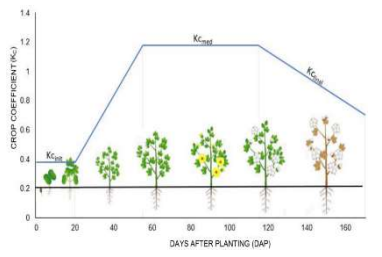
FIGURE 1. Location of the study area and identification of the center pivots.

Effective evapotranspiration (ET<sub>r</sub>) was estimated from images obtained through the Landsat 7 (ETM+ sensor) and Landsat 8 (OLI sensor) satellites, one at the beginning of each cotton phenological stage (Table 1). Both sensors have a spatial resolution of 30 m. Climatic data (air temperature [T<sub>m</sub>, °C], wind speed at 2 m height [WS, m·s<sup>-1</sup>], radiation [Ra, MJ m<sup>2</sup>·day<sup>-1</sup>], relative humidity [RH, %], and rainfall [R, mm]), which are necessary to assist in the calibration of the ET<sub>r</sub> models (calculated by the Penman–Monteith method [PM-FAO 56] (Allen et al., 1998), were obtained through an automatic meteorological station located near the center pivots and granted by the Brazilian company

IRRIGER - Irrigation management and engineering (<http://www.irriger.com.br/en-US/>) (Figure 1).

The crop coefficient (K<sub>c</sub>) represents the integration of the effects of three characteristics (crop height, surface resistance, and crop-soil surface albedo) (Pokorny, 2019), which varies according to the phenological stages of the crop, with the possibility of being affected by the duration of the phenological stages (Venancio et al., 2020), and is applied in irrigation management and water allocation (Rozenstein et al., 2019). Therefore, the K<sub>c</sub> applied by IRRIGER for irrigation management in commercial areas is based on the recommendations of FAO-56 (Allen et al., 1998); in this sense, the K<sub>c</sub> values for the initial, medium, and final stages were 0.38, 1.2, and 0.8, respectively (Table 1).

TABLE 1. Dates of the satellite images used in the study for the three agricultural years.

Phenological Stages	Satellite	Sensor	Size pixel	Image date	Julian Day	Crop coefficient (K <sub>c</sub> )*
I	Landsat 7	ETM+	30 m	1/17/2018	17	
II	Landsat 8	OLI		2/10/2018	41	
III	Landsat 7	ETM+		4/23/2018	113	
IV	Landsat 8	OLI		5/17/2018	137	
I	Landsat 8	OLI		1/12/2019	12	
II	Landsat 8	OLI		2/13/2019	44	
III	Landsat 8	OLI		4/18/2019	108	
IV	Landsat 7	ETM+		5/12/2019	132	
I	Landsat 8	OLI		1/15/2020	15	
II	Landsat 8	OLI		3/19/2020	79	
III	Landsat 7	ETM+		4/12/2020	103	
IV	Landsat 7	ETM+		5/30/2020	151	

### Application of algorithms to measure ET<sub>r</sub>

To present alternatives for calculating ET<sub>r</sub>, considering the evaluation of efficiency and ease of obtaining data to perform ET<sub>r</sub> estimates, three ET<sub>r</sub> estimation methods were applied in this study:

1) **Surface Energy Balance Algorithm for Land (SEBAL)**: A method proposed by Bastiaanssen et al. (1998) to empirically measure the spatial variation of most essential hydrometeorological parameters, requiring only field information on short-wave atmospheric transmittance, surface temperature, and vegetation height. A simplified form of the SEBAL algorithm is shown in eqs (1), (2) and (3).

$$\lambda ET = (R_n - G - H) \quad (1)$$

$$ET_{inst} = 3,600 / (\lambda ET - \lambda) \quad (2)$$

$$ET_{24} = ET_r F \times ET_{r,24} \quad (3)$$

Where:

LE = latent energy consumed by ET;

R<sub>n</sub> = net radiation resulting from the sum of all incoming and outgoing short-wave and long-wave radiation on the surface;

G = sensitive heat flux conducted to the soil;

H = sensitive heat flux converted to the air;

ET<sub>inst</sub> = instantaneous ET (mm·h<sup>-1</sup>);

3,600 second-to-hour conversions;

ET<sub>24</sub> = 24-hour evapotranspiration;

λET = latent heat flux (W·m<sup>-2</sup>);

λ = latent vaporization heat (J·kg<sup>-1</sup>);

ET<sub>r</sub>F = reference ET fraction, and

ET<sub>r,24</sub> = daily ET<sub>r</sub>.

### 2) Mapping Evapotranspiration at High Resolution and with Internalized Calibration (METRIC)

(Allen et al., 2007): This method was implemented on the Google Earth Engine platform, being called Earth Engine Evapotranspiration Flux (EEFlux) and available for processed images from the Landsat 7 and 8 satellites (Allen et al., 2015). A simplified demonstration of METRIC is shown in eqs (4), (5) and (6).

$$ET_{inst} = 3600(LE / \lambda \rho_w) \quad (4)$$

$$\lambda = [2.501 - 0.00236(T_s - 273.15)] \times 10^6 \quad (5)$$

$$ET_r F = ET_{inst} / ET_r \quad (6)$$

Where:

ET<sub>inst</sub> = instantaneous ET (mm·h<sup>-1</sup>);

$LE$  = latent heat flux ( $W \cdot m^{-2}$ );

$\rho_w$  = water density (approximately  $1,000 \text{ kg} \cdot m^{-3}$ );

$\lambda$  = vaporization latent ( $J \cdot kg^{-1}$ ) represents the heat absorbed when 1 kg of water evaporates and is calculated;

$ET_r F$  = fraction of the reference ET ( $ET_r$ ), it is for the 0.5 m height standardized alfalfa reference at the time of the image,

$T_s$  = surface temperature (K).

**3) Simple Algorithm for Evapotranspiration Retrieving (SAFER)** (Teixeira, 2010): It uses satellite images to determine the normalized difference vegetation index (NDVI), surface albedo ( $S_a$ ), and surface temperature ( $T_0$ ) parameters. The equation for calculating  $ET_r$  is shown in a simplified form in [eq. (7)].

$$ET_r = \exp \left[ a_{sf} + b_{sf} \left( \frac{T_0}{\alpha_0 NDVI} \right) \right] \quad (7)$$

Where:

$\lambda$ : vaporization latent ( $J \cdot kg^{-1}$ ) represents the heat absorbed when 1 kg of water evaporates and is calculated as in the equation;

$a$  and  $b$  are regression coefficients;

where  $a_{sf} = 1$  and  $b_{sf} = -0.008$ ;

$T_0$ : surface temperature;

$\alpha_0$ : surface albedo, and

NDVI: Normalized Difference Vegetation Index.

### Protocol applied for construction of irrigation management zones

IMZs were determined from the  $ET_r$  data for each of the three  $ET_r$  estimation methods (SEBAL, METRIC, and SAFER). The IMZs were generated from an orbital image obtained at different phenological stages of the crop, which served as the basis for calculating  $ET_r$ , thus having an irrigation map for each crop stage, represented by the map of the IMZ generated. Figure 2 shows the evaluation of the stages and processing steps performed to obtain IMZs.

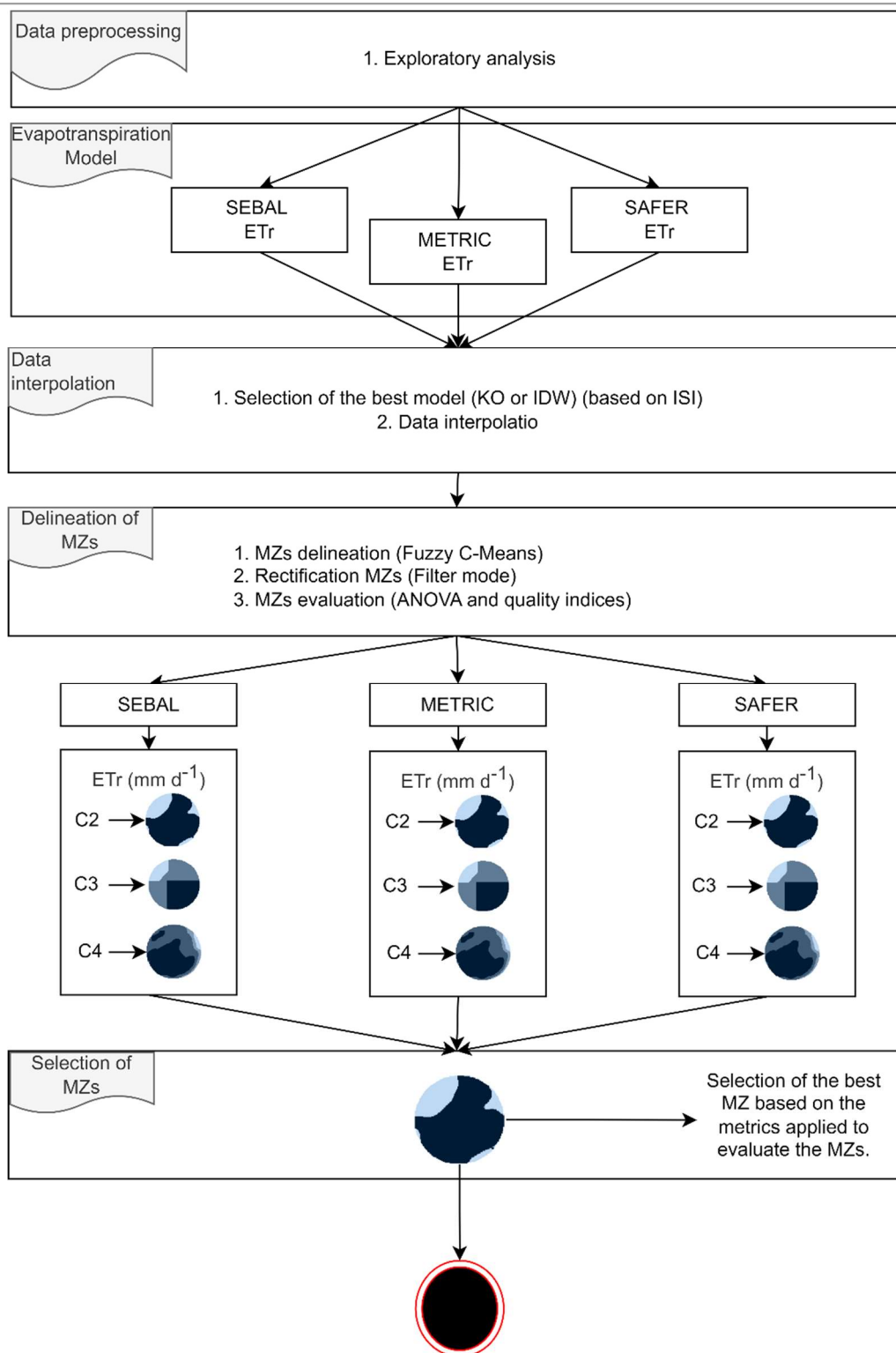


FIGURE 2. Flowchart for the generation of irrigation management zones (IMZs) with algorithm data. Acronyms: C2, C3, C4, management zones with two, three, and four classes respectively; effective evapotranspiration (ETr); index of interpolator selection (ISI).

**Data Processing:** Descriptive and exploratory statistical analyses were performed, which were classified according to Pimentel-Gomes (2009), and boxplot graphs were created.

**Evapotranspiration Model (ETr mm·d<sup>-1</sup>):** The ETr data were obtained from the calculations applied to the four selected satellite images representing the beginning of each development stage. The models used are

SEBAL (Equation 2), METRIC (Equation 4), and SAFER (Equation 7).

**Data interpolation:** Spatial interpolation methods are classified into deterministic methods (e.g., inverse of the distance to a power method-IDW), geostatistical methods (e.g., ordinary kriging-OK, cokriging-COK), and hybrids (Shen et al., 2019). These aim to cover unsampled areas from the raw data interpolated to a denser grid, which can

create smooth and continuous MZs. In this study, the data were interpolated using the AgDatabox-Map platform (ADB-Map, <https://adb.md.utfpr.edu.br/>), and a computational routine capable of identifying the best interpolation method and parameters for (OK) was implemented, as well as the best exponent to be used in the inverse distance method raised to power (IDW) (Betzek et al., 2018). The choice of power is given through cross-validation (mean error = ME, Equation 8, and the standard deviation of the mean errors =  $SD_{ME}$ , Equation 9), and lowest index of interpolator selection (ISI, Equation 10; (Bier & Souza, 2017).

$$ME = \frac{1}{n} \sum_{i=1}^n (z(s_i) - \hat{z}(s_i)) \quad (8)$$

$$SD_{ME} = \sqrt{\frac{1}{n} \sum_{i=1}^n (z(s_i) - \hat{z}(s_i))^2} \quad (9)$$

$$ISI = \left\{ \frac{abs(ME)}{\max_{i=j^j}[abs(ME)]} + \frac{[SD_{ME} - \min_{i=j^j}(SD_{ME})]}{\max_{i=j^j}[abs(DP_{ME})]} \right\} \quad (10)$$

Where:

$ME$  is the mean error;

$SD_{ME}$  is the standard deviation of the mean errors;

$n$  is the number of data;

$Z(s_i)$  is the value observed at point  $s_i$ ;

$\hat{z}(s_i)$  is the value predicted by kriging at point  $s_i$ ;

$abs(ME)$  is the module value of the cross-validation mean error;

$\min_{i=j^j}$  is the lowest value found among the  $j$  models compared, and

$\max_{i=j^j}$  is the highest value found among the  $j$  models compared.

**Rectification of maps:** It is necessary to remove blemishes from small or isolated pixels. For this purpose, filters were applied to smooth the isolated pixels with the function of reducing class fragmentation (Ping & Dobermann, 2003). Studies developed by Betzek et al. (2018) recommended a median with a mask ( $5 \times 5$ ), which presented a better performance. A median filter with a  $5 \times 5$  mask was used.

**Assessment of the irrigation management zone:**

The delineated IMZs were evaluated using the mean test and statistical methods.

1) Tukey's test at 5% probability was used to assess the grouping of classes in the management zones;

2) Variance reduction (VR) (Ping & Dobermann, 2003): which represents the reduction in the variance percentage when dividing the area into MZs (Equation 11).

$$VR = \left( 1 - \frac{\sum_{i=1}^c W_i * V_{MZi}}{V_{field}} \right) * 100 \quad (11)$$

Where:

$c$  is the number of MZs,

$W_i$  is the proportion of the total area referring to the  $i^{\text{th}}$  MZ,

$V_{MZi}$  is the data variance of the  $i^{\text{th}}$  MZ, and

$V_{field}$  is the data variance of the area as a whole.

3) Fuzzy performance index (FPI) (Fridgen et al., 2004): It estimates the degree of separation between classes (Equation 12). This index varies between 0 and 1 and when it is closer to 0, the classes become more distinct, with less member sharing (Yao et al., 2014). Studied developed by Schenatto et al. (2017) applied the FPI to evaluate MZs delineated by the Fuzzy C-Means algorithm to obtain good results.

$$FPI = 1 - \frac{c}{c-1} \left[ 1 - \sum_{j=1}^n \sum_{i=1}^c (u_{ij})^2 / n \right] \quad (12)$$

where:

$c$  is the number of classes (clusters);

$n$  is the sample size for the entire area (number of observations), and

$u_{ij}$  is the  $ij$  element of the fuzzy pertinence matrix.

4) Modified Entropy Partition (MPE) (Boydell & Mcbratney, 2002, Equation 13): It estimates the disorganization created by a specific number of classes, varying from 0 to 1. When a value is closer to 1, disorganization predominates, while values close to 0 indicate excellent organization (Fridgen et al., 2000).

$$MPE = \frac{-\sum_{j=1}^n \sum_{i=1}^c u_{ij} \log(u_{ij}) / n}{\log c} \quad (13)$$

Where:

$c$  is the number of classes (clusters);

$n$  is the sample size for the entire area (number of observations), and

$u_{ij}$  is the  $ij$  elements of the fuzzy pertinence matrix.

5) Average silhouette coefficient (ASC) (Rousseeuw, 1987, Equation 14): The ASC coefficient was obtained from the silhouette coefficient (SC), which is an evaluation index that measures both the level of satisfactory internal formation and external separation of groups. The SC value for point  $p$ , denoted by  $sc_p$ , is calculated using the average of the intra-group distances  $a_p$  and the average of the inter-group distances  $b_p$ :

$$SCp = \frac{b_p a_p}{\max(a_p, b_p)} \quad (14)$$

Where:

$a_p$  is the average of the distances between point  $p$  and all other points in the same group, and

$b_p$  is the average of the distances between point  $p$  and all points in the closest group that contains  $p$ .

Quantum GIS (QGIS Development Team, 2021) and AgDataBox Map (Bazzi et al., 2019; Michelon et al., 2019) software programs were used for data processing and statistical analysis.

### Cost analysis

A cost analysis was performed for the IMZs that presented the best evaluation indices Equations 15–18. In this analysis, a fixed cost of R\$2.00 per millimeter per hectare of applied water was established. This value practiced in the western region of Bahia includes all administrative and governmental charges.

$$C = \underline{ETr} * B \quad (15)$$

$$CA = C * A \quad (16)$$

$$D = \sum CA - FR \quad (17)$$

$$FR = \underline{ETr} * B * A_{class} \quad (18)$$

Where:

$C$  is the cost per millimeter applied in each class;

$ETr$  is the average observed in every irrigated pivot;

$A$  is the area in hectares;

$B$  is the cost to apply 1 mL of water, a value considered standard 2;

$CA$  is the cost to apply to each class;

$D$  is the sum of the cost per area for all classes minus the value observed in the fixed rate ( $FR$ );

$FR$  is the cost to irrigate 1 mL at a fixed rate over the entire irrigated area;

Class is the area of each class.

## RESULTS AND DISCUSSION

The seasonal behavior of the meteorological variables for the three cotton harvest years (2018, 2019, and 2020) is presented in Figure 3. During the period from January 9<sup>th</sup> to April 25<sup>th</sup> (phenological stages I, II, and III), there was the highest rainfall volume, which corresponded to a mean above 95% (747.83 mm) of all rainfall in the cotton cycle for the three agricultural years. From this period onwards, water supplementation through irrigation should occur to complete the cotton cycle without major losses in productivity. Second, Rosolem (2001) reported that during maturation of apples, which corresponds to stages III to IV, lack of water causes production of inferior quality fibers. Corroborating the results observed for rainfall, it is important to highlight that the complete cotton cycle, which corresponded to 170 days, presented an overall mean  $ET_o$  (three years) of 627.72 mm, with 56% of this volume evapotranspirated in cotton stages II and III.

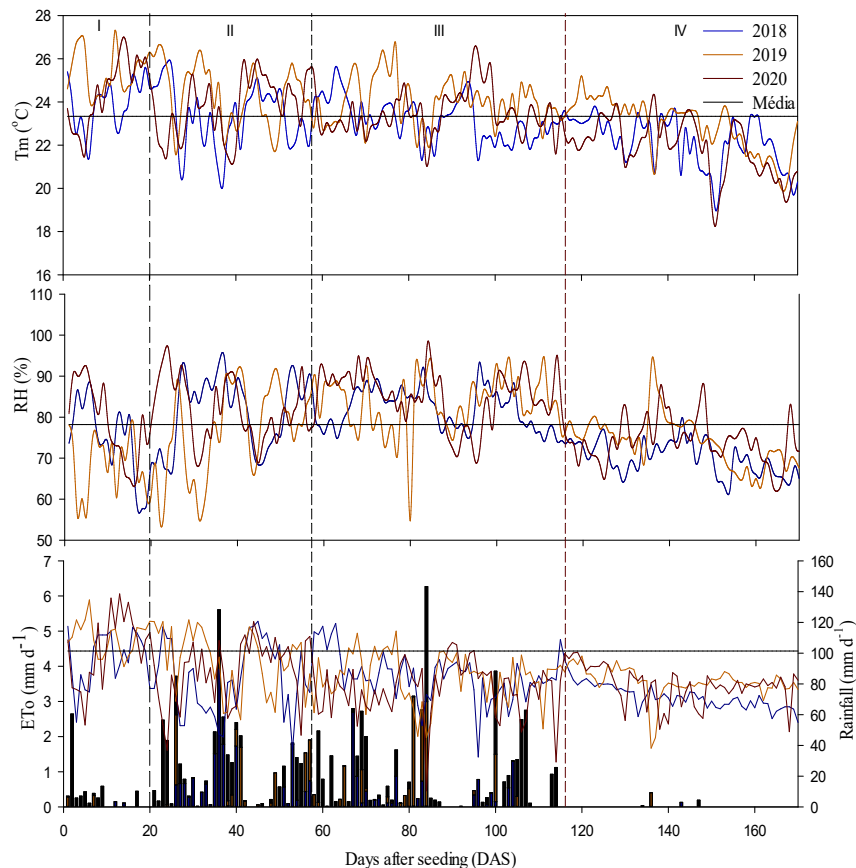


FIGURE 3. Meteorological data: mean daily temperature ( $T_m$ ; °C), relative humidity ( $RH$ ; %), rainfall ( $R$ ;  $\text{mm} \cdot \text{d}^{-1}$ ), and reference evapotranspiration ( $ET_o$ ;  $\text{mm} \cdot \text{d}^{-1}$ ) during the cotton 2018, 2019 and 2020 harvest years.

Studies by Bezerra et al. (2010) with the BRS-200 brown cotton cultivar showed ETr values of 3.8, 5.0, 5.9, and 5.4 mm·d<sup>-1</sup> for stages I, II, III, and IV of the phenological cycle, respectively. Rosolem (2001) highlighted that in the phase corresponding to the first flora to the first boll, the water requirement increases from 4 mm·day<sup>-1</sup> to more than 8 mm·day<sup>-1</sup>, following the development of leaves.

The rainy season in this region experienced rainfall according to recommended intervals. However, in the final phase of the cotton cycle there was a reduction to < 9.2 mm

of rain a month; this represents less than 2% of the entire rainfall volume throughout the cotton cycle, requiring supplementation via irrigation. Thus, optimal and consistent yields are usually obtained through irrigation (Pershing et al., 2012).

Figure 4 presents the time distribution of ETr as a function of its respective cotton growth stage for the three methods under study (METRIC, SAFER, and SEBAL). According to studies by Del Grosso et al. (2018), ETr was positively correlated with NDVI and proved that as NDVI increased.

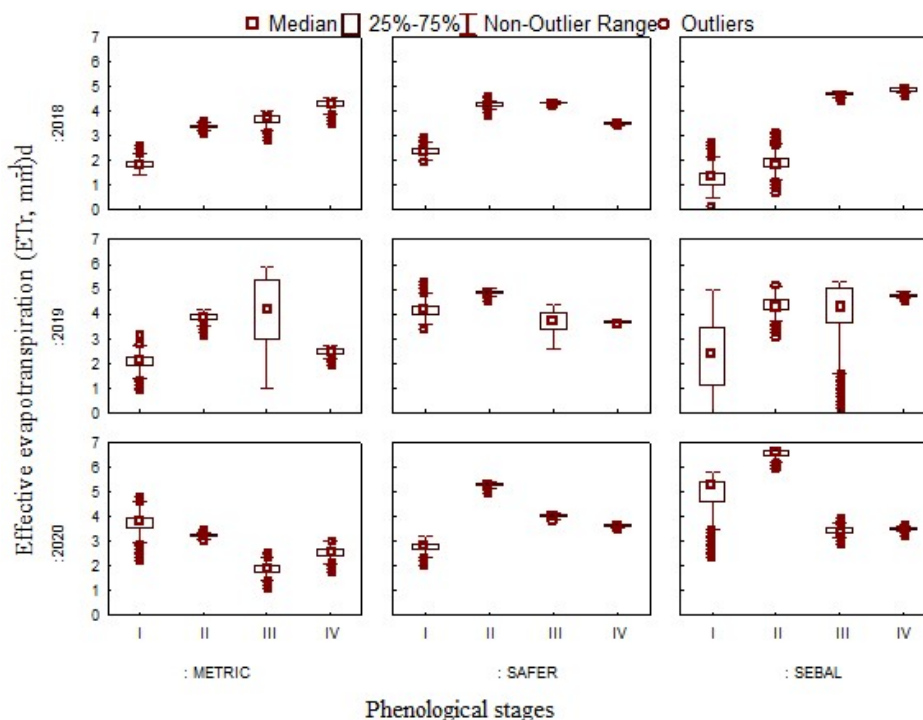


FIGURE 4. Boxplot of effective evapotranspiration (ETr, mm·d<sup>-1</sup>) for each estimation model (METRIC, SAFER, and SEBAL) at different cotton phenological stages (I, II, III, and IV).

Spatial variability of ETr was observed along the study area for the three ETr estimation methods (SEBAL, METRIC, and SAFER). The interpolation of the ETr data was based on the cross-validation proposed by Bier & Souza (2017), and as observed, the most predominant method was OK. Interpolated ETr maps for each physiological stage are presented (Table 1S). Maps with higher fragmentation numbers are characteristic of interpolation with IDW (Figures 1S).

Figures 5 present the IMZs delineated from the ETr data in three estimation methods (SEBAL, METRIC, and SAFER). The aforementioned IMZs were separated according to the phenological stages (I, II, III, and IV) of the cotton crop in three agricultural years. It can be observed that, in stages I and IV, the IMZs and the divisions by classes present a concentration in a given class. In addition to that, the SEBAL and SAFER methods present greater fragmentation of IMZs in 2019, causing further rectifications.

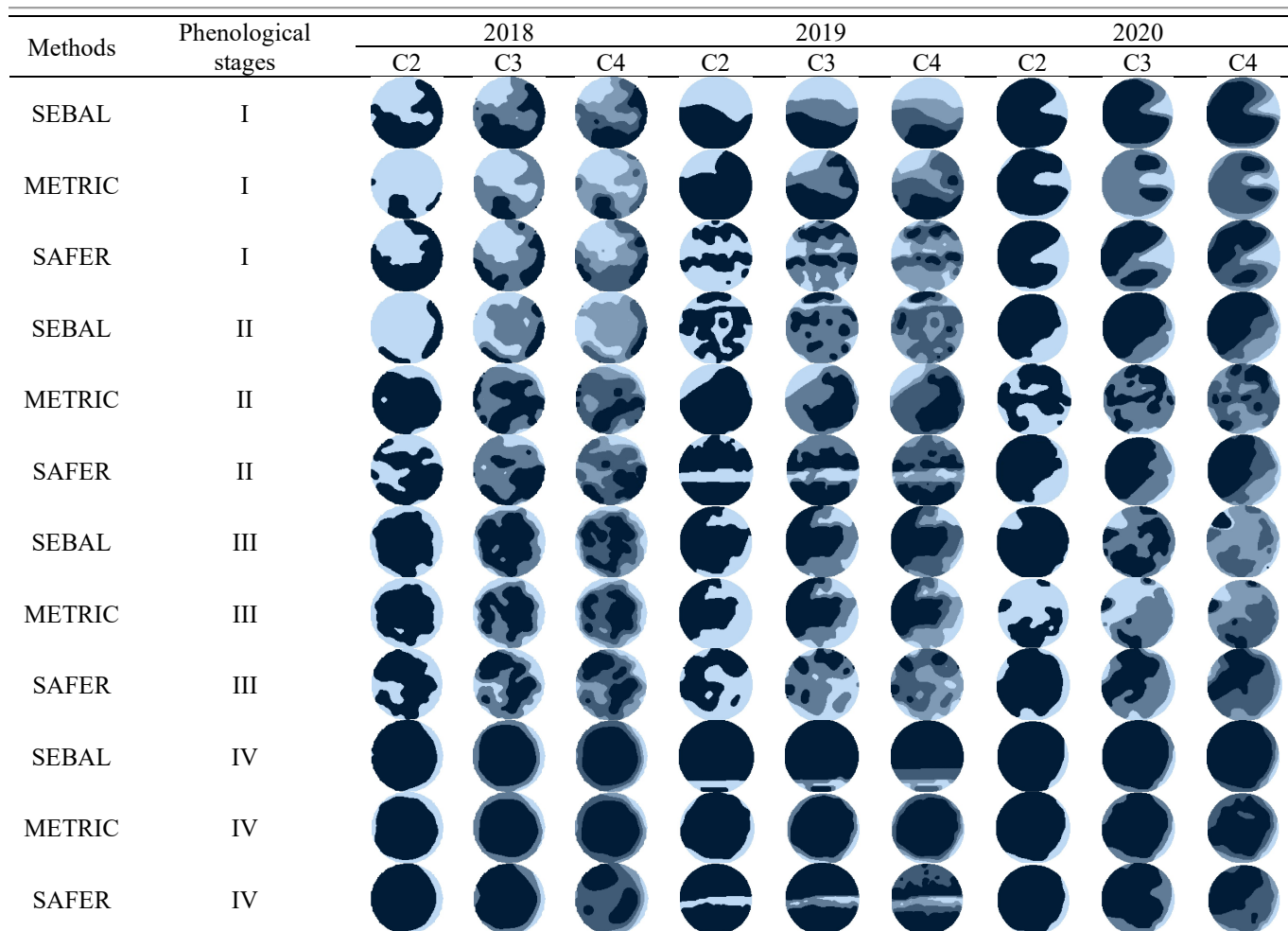


FIGURE 5. Management zones generated according to the ETr methods (METRIC, SAFER, and SEBAL) for the different phenological stages of cotton (I, II, III, and IV) for the 2020 cotton harvest year. \*All the IMZs were rectified through the median method.

The IMZs were evaluated using the mean test (Tukey's) and the ASC, FPI, MPE, and VR% indices (Table 2 and Figure 5). This proposal shows that despite the small differences between the ETr values, it is

possible to identify that the IMZs show statistical differences using Tukey's test (Table 2). Based on this result, a precision mechanism can be used, according to Fontanet et al. (2020), to predict the need for management.

TABLE 2. Mean test and evaluation indices for IMZs from the effective evapotranspiration estimated by three models (METRIC, SEBAL, and SAFER) for the center pivot with cotton cultivation in the 2018, 2019, and 2020 harvest years.

Year	Method	Stage	N Classes	Tukey's test				ASC	FPI	MPE	VR%	
				C1	C2	C3	C4					
2018	SEBAL	I	2	0.9a	1.5b			0.62	0.067	0.080	74	
			3	0.7a	1.1b	1.6c		0.57	0.082	0.083	87	
			4	0.6a	1.0b	1.4c	1.7d	0.61	0.059	0.053	94	
	METRIC		2	1.8a	2.4b			0.69	0.042	0.051	68	
			3	1.6a	1.9b	2.5c		0.58	0.061	0.063	85	
			4	1.6a	1.8b	2.1c	2.5d	0.56	0.066	0.060	90	
	SAFER		2	2.2a	2.4b			0.60	0.080	0.095	68	
			3	2.2a	2.3b	2.5c		0.54	0.081	0.082	82	
			4	2.2a	2.3b	2.4c	2.5d	0.54	0.074	0.067	88	
	SEBAL		II	2	1.8a	2.6b			0.68	0.038	0.047	57
				3	1.6a	2.0b	2.8c		0.52	0.086	0.087	75
				4	1.5a	1.9b	2.3c	3.2d	0.54	0.074	0.067	82
	METRIC	2		3.2a	3.4b			0.60	0.078	0.095	58	
		3		3.1a	3.3b	3.4c		0.54	0.078	0.079	81	
		4		3.1a	3.3b	3.3c	3.4d	0.50	0.093	0.083	88	
	SAFER	2		4.1a	4.3b			0.51	0.116	0.138	54	
		3		4.0a	4.2b	4.3c		0.54	0.080	0.081	73	
		4		4.0a	4.1b	4.2c	4.3d	0.50	0.093	0.080	81	
	SEBAL	III		2	4.6a	4.7b			0.64	0.066	0.079	69
				3	4.5a	4.6b	4.7b		0.59	0.062	0.068	84
				4	4.5a	4.6b	4.7c	4.7c	0.53	0.084	0.075	90
	METRIC		2	3.5a	3.8b			0.63	0.067	0.080	72	
			3	3.5a	3.6b	3.8c		0.57	0.074	0.074	87	
			4	3.4a	3.6b	3.7c	3.8d	0.55	0.070	0.068	91	
SAFER	2		4.2a	4.3b			0.61	0.072	0.087	69		
	3		4.2a	4.3b	4.3b		0.54	0.089	0.089	83		
	4		4.2a	4.3b	4.3b	4.3b	0.55	0.073	0.066	90		
SEBAL	IV		2	4.4a	4.8b			0.76	0.036	0.043	70	
			3	4.3a	4.7b	4.9b		0.69	0.048	0.048	88	
			4	4.2a	4.5b	4.7c	4.9d	0.68	0.047	0.041	90	
METRIC		2	3.6a	4.3b			0.69	0.070	0.082	66		
		3	3.1a	3.9b	4.3c		0.70	0.047	0.047	84		
		4	2.9a	3.6b	4.0c	4.3d	0.68	0.045	0.041	91		
SAFER		2	3.3a	3.5b			0.76	0.031	0.038	61		
		3	3.3a	3.4b	3.5c		0.65	0.043	0.044	79		
		4	3.2a	3.4b	3.5c	3.5c	0.54	0.073	0.067	84		
2019		SEBAL	I	2	1.1a	3.4b			0.62	0.084	0.098	75
				3	0.6a	2.2b	3.7c		0.62	0.057	0.058	90
				4	0.6a	1.9b	2.1c	4.0d	0.59	0.060	0.057	94
	METRIC	2		1.4a	2.2b			0.70	0.041	0.049	71	
		3		1.3a	1.9b	2.3c		0.56	0.078	0.078	86	
		4		1.2a	1.8b	2.1c	2.4d	0.54	0.082	0.074	91	
	SAFER	2		4.1a	4.3b			0.61	0.068	0.083	68	
		3		4.1a	4.2b	4.3c		0.54	0.083	0.084	83	
		4		4.0a	4.1b	4.2c	4.3d	0.54	0.076	0.069	89	
	SEBAL	II		2	4.3a	4.4b			0.54	0.099	0.119	62
				3	4.2a	4.3b	4.5c		0.53	0.090	0.091	79
				4	4.2a	4.3b	4.4c	4.5d	0.53	0.089	0.080	87
	METRIC		2	3.5a	3.9b			0.72	0.028	0.034	75	
			3	3.5a	3.8b	4.0c		0.60	0.065	0.065	89	
			4	3.4a	3.6b	3.9c	4.0d	0.59	0.063	0.057	93	
	SAFER		2	4.8a	4.9b			0.63	0.066	0.080	68	
			3	4.7a	4.8b	4.9c		0.57	0.072	0.072	83	
			4	4.7a	4.8b	4.9c	4.9c	0.55	0.078	0.070	90	
	SEBAL		III	2	2.6a	4.6b			0.63	0.075	0.091	68
				3	2.1a	3.7b	4.9c		0.67	0.052	0.052	89

Year	Method	Stage	N Classes	Tukey's test				ASC	FPI	MPE	VR%
				C1	C2	C3	C4				
				-----mm·d <sup>-1</sup> -----							
2020	METRIC		4	1.6a	2.9b	3.9c	4.9d	0.67	0.054	0.048	95
			2	2.9a	5.2b			0.73	0.042	0.050	84
			3	2.5a	3.5b	5.3c		0.63	0.070	0.071	91
			4	2.3a	3.2b	4.3c	5.4d	0.65	0.054	0.049	96
	SAFER		2	3.6a	3.8b			0.59	0.083	0.100	67
			3	3.6a	3.7b	3.8c		0.53	0.095	0.094	81
			4	3.5a	3.6b	3.7c	3.8d	0.52	0.091	0.081	88
			<hr/>								
	SEBAL		2	4.1a	4.8b			0.88	0.011	0.014	83
			3	3.9a	4.4b	4.8c		0.84	0.018	0.018	93
			4	3.9a	4.3b	4.7c	4.8d	0.63	0.025	0.027	96
			<hr/>								
	METRIC	IV	2	1.8a	2.3b	2.5c		0.71	0.041	0.042	86
			3	1.8a	2.3b	2.5c		0.71	0.041	0.042	86
			4	1.7a	2.1b	2.3c	2.5d	0.66	0.041	0.038	91
			<hr/>								
	SAFER		2	3.6a	3.7b			0.78	0.031	0.037	76
			3	3.5a	3.6b	3.7c		0.53	0.084	0.075	92
			4	3.5a	3.6b	3.7c	3.7c	0.72	0.031	0.032	88
			<hr/>								
SEBAL		2	2.3a	5.1b			0.77	0.047	0.054	74	
		3	1.6a	3.9b	5.3c		0.72	0.039	0.039	91	
		4	1.5a	3.5b	4.6c	5.4d	0.66	0.050	0.045	94	
		<hr/>									
METRIC	I	2	3.1a	4.0b			0.64	0.061	0.074	64	
		3	3.1a	3.8b	4.4c		0.60	0.059	0.061	80	
		4	2.8a	3.4b	3.9c	4.4d	0.60	0.062	0.056	89	
		<hr/>									
SAFER		2	2.5a	2.9b			0.69	0.049	0.058	75	
		3	3.1a	4.9b	5.2c		0.60	0.075	0.075	89	
		4	2.4a	2.6b	2.8c	2.9d	0.60	0.059	0.053	94	
		<hr/>									
SEBAL		2	6.4a	6.6b			0.73	0.038	0.046	75	
		3	6.2a	6.4b	6.6c		0.70	0.044	0.044	87	
		4	3.4a	4.2b	4.7c	5.1c	0.63	0.051	0.046	92	
		<hr/>									
METRIC	II	2	3.2a	3.3b			0.52	0.113	0.135	51	
		3	3.1a	3.2c	3.3c		0.54	0.083	0.084	71	
		4	3.1a	3.2b	3.2b	3.3c	0.54	0.078	0.071	82	
		<hr/>									
SAFER		2	5.2a	5.5b			0.65	0.073	0.087	65	
		3	5.1a	5.3b	5.4c		0.66	0.050	0.050	86	
		4	5.1a	5.2b	5.3c	5.4d	0.61	0.051	0.047	91	
		<hr/>									
SEBAL		2	2.6a	3.5b			0.82	0.020	0.023	73	
		3	2.5a	3.3b	3.5c		0.48	0.098	0.101	82	
		4	2.3a	3.0b	3.4c	3.6d	0.55	0.074	0.067	90	
		<hr/>									
METRIC	III	2	1.8a	2.1b			0.51	0.126	0.152	50	
		3	1.7a	1.9b	2.3c		0.54	0.084	0.086	74	
		4	1.5a	1.8b	2.0c	2.4d	0.57	0.064	0.059	83	
		<hr/>									
SAFER		2	3.9a	4.1b			0.68	0.048	0.057	61	
		3	3.8a	4.0b	4.1c		0.55	0.087	0.088	74	
		4	3.8a	3.9b	4.0c	4.1d	0.59	0.070	0.062	86	
		<hr/>									
SEBAL		2	2.4a	3.5b			0.87	0.018	0.022	70	
		3	2.1a	3.2b	3.5c		0.81	0.023	0.024	88	
		4	1.9a	2.7b	3.3c	3.5d	0.80	0.023	0.020	86	
		<hr/>									
METRIC	IV	2	1.9a	2.6b			0.75	0.037	0.045	62	
		3	1.5a	2.3b	2.6c		0.67	0.043	0.044	81	
		4	1.4a	2.2b	2.5c	2.7d	0.56	0.069	0.063	87	
		<hr/>									
SAFER		2	3.4a	3.7b			0.77	0.031	0.037	64	
		3	3.3a	3.6b	3.7c		0.61	0.055	0.057	84	
		4	3.3a	3.5b	3.6c	3.7d	0.60	0.063	0.057	88	
		<hr/>									

\*Management zones followed by different letters differ from each other according to Tukey's test at 5% probability of error; VR% = variance reduction; ASC = Average silhouette coefficient; FPI = Fuzzy performance index; MPE = Modified partition entropy index.

To select the best IMZs, application of the indices becomes a key parameter to determine whether the grouping was carried out effectively. Therefore, considering the variance reduction (VR) to choose the best IMZs for irrigation management in each phenological phase, an increase could be observed as the number of classes increased with a clearer trend when the IMZs were generated with ETr data from METRIC. In contrast, there was a reduction across years and in the phenological phases for the SEBAL and SAFER data (Table 2).

SEBAL presented a reduction in stages II and IV in 2020; zones with three classes are recommended; however, in the other phases and years, IMZs with four classes are the most suitable for irrigation management. For the IMZs generated with SAFER data, there was a reduction in the VR in 2018 in stage IV, indicating the application of the IMZs with two classes, whereas for the other phases and years under study, it is recommended that IMZs be applied with four classes (Table 2, Figure 6).

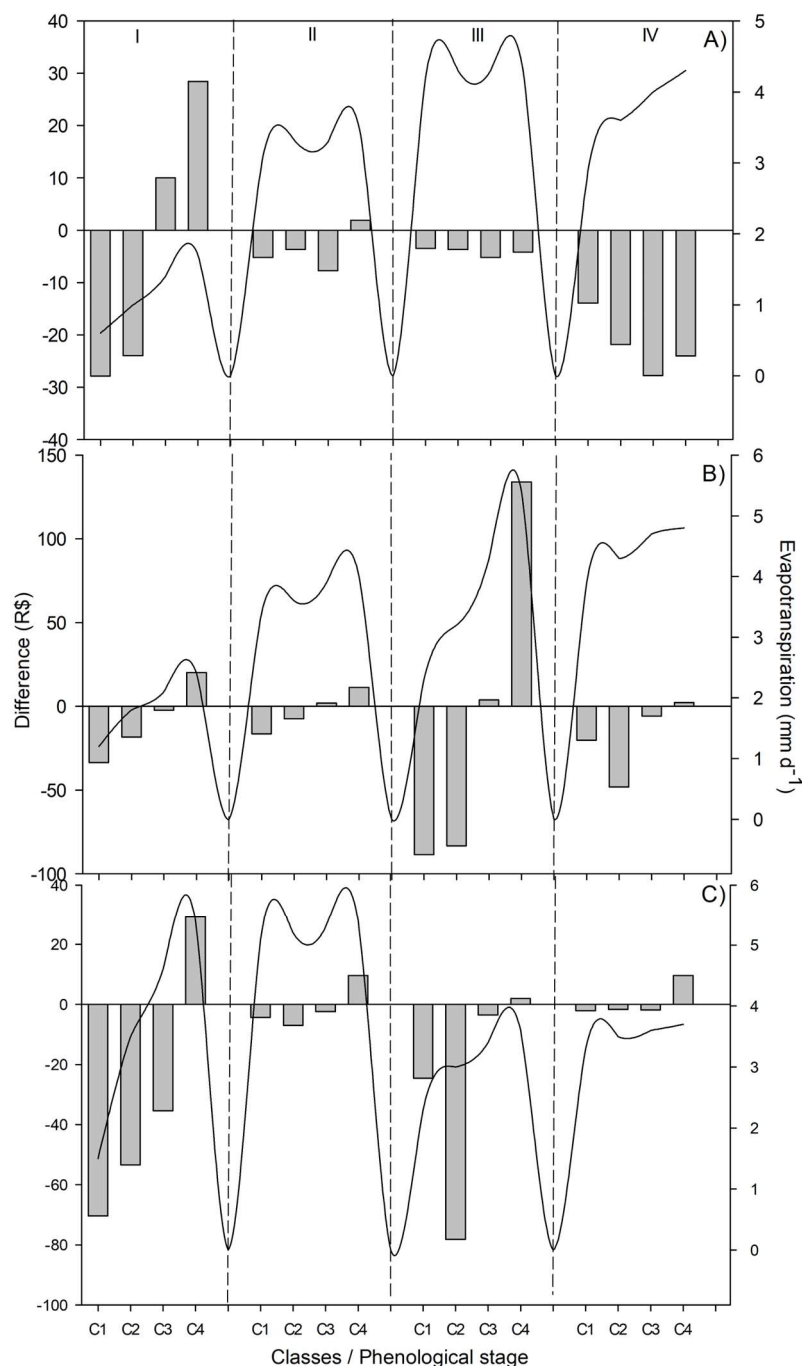


FIGURE 6. Irrigation cost evaluation for selected IMZs based on VR indices in the four phenological stages and for the three harvest years: (A) 2018, (B) 2019, and (C) 2020. Classes is the amount of water applied in the evaluated class (C1, C2, C3, and C4); Fixed rate is the cost to uniformly apply in an area; and Difference (R\$) is the cost for fixed rate application - the application cost between each class for each phenological stage (I, II, III and IV).

Management of variable rate irrigation (VRI) is divided into several techniques; however, for the management of center pivots, two techniques are applied: speed control and control of VRI zones. Speed control is a viable technique from an economic point of view, considering that in areas that already have pivots installed, it is possible to optimize water use by employing the speed of each sector (Morais et al., 2019).

Decision support systems for irrigation and water conservation are used to minimize water application and maximize production (Mendes et al., 2019). Irrigation management based on IMZs can be a viable technique from a practical point of view, avoiding the need for producers to purchase new irrigation systems to apply precision agriculture techniques. It is common in other field activities, such as fertilizer and phytosanitary applications, to use traditional application equipment to carry out localized management without the need to purchase new equipment that performs variable-rate application. This occurs through the definition of zones according to the chemical, physical, and biological characteristics of the soil, plants, and atmosphere.

A proposal based on this principle was suggested by Mendes et al. (2019), who recommended the application of the fuzzy algorithm to define MZs using RS data to calculate the NDVI, canopy temperature, and soil moisture in the upper layer. In addition, each image used was considered during the development stage of the culture. The proposal suggested in this study was to use ETr data to group the sampling points and classify the best number of IMZs for irrigation management.

This article suggests the application of VRI based on the control of the variable irrigation application rate on the pivot, proposing a division with up to four classes for the best operation of the irrigation system. Therefore, the best IMZs were selected based on the VR for each year (Figure 5). To compare the irrigation management strategies, a comparison was made between a uniform application (fixed rate) and the best IMZs. Therefore, in all years and phenological stages, classes C1, C2, and C3 showed lower ETr and concentrated a mean of 60% of the entire irrigated area, which required lower water consumption according to crop demand when compared to the rest of the field. Despite the relatively low financial impact, the productivity of class C4 may have been harmed by the lack of water during the different phenological stages, especially stages III and IV. In addition, it was verified through the analyses conducted that the water made available in excess in regions C1 and C2 could be managed in regions where the water deficit was greater (C4), maintaining consumption but with more efficient management. From the perspective of crop development, it is important to verify the needs arising from the phases of crop development and the need for localized management according to the need for each IMZ.

Notably, the irrigation zones were not stable during the phenological phases of the crop and the evaluated crops differed in terms of the ETr estimation method, having a dynamic aspect and with a constant need to update the configuration procedures of the irrigation systems.

## CONCLUSIONS

It was possible to delineate IMZs based on data from three ETr estimation algorithms (METRIC, SEBA, and SAFER). SEBAL was the method that best presented data groupings for the three agricultural years, although all methods generated IMZs with field applicability. The ease in obtaining the METRIC data allows for an easier procedure to generate the IMZs, compared to the data obtained from SEBAL, which presents greater complexity in its initial processing. The SAFER method, which was developed for the semi-arid Brazilian region, provided satisfactory results for the delineation of IMZs in cotton crops.

The delineation of IMZs with ETr data is a viable alternative from technical and operational points of view, for smart irrigation and to reduce costs. The groupings performed had selection of IMZs of two, three and four zones, where there was a mean cost reduction of R\$ 9.55 per millimeter applied across the three agricultural years, which shows the importance of evaluating irrigation management considering spatial variability to economic and environmental ways. Classes C1, C2, and C3 presented lower ETr and concentrated a mean of 60% of the entire irrigated area, which required lower water consumption than crop demand. ETr methods may be applied to optimize water use, without increasing the expenses (economic viability).

The product generated in this research can be made available to the producers to carry out irrigation management in a different way in their irrigated area, considering two and three different zones that will yield different levels.

In general, the work contributed to the evaluation of ETr estimation methods to define irrigation zones that can be utilized as strategies for localized irrigation, providing water savings and cost reduction.

## ACKNOWLEDGEMENTS

The authors are grateful to the Western Paraná State University (UNIOESTE), Technological Federal University of Paraná (UTFPR), Coordination for the Improvement of Higher Education Personnel (CAPES), National Council for Scientific and Technological Development (CNPq), and Itaipu Technological Park Foundation (FPTI) for the support received.

## REFERENCES (ref. corrigidas/ faltam citações)

- Ahmad U, Alvino A, Marino S (2021) A Review of Crop Water Stress Assessment Using Remote Sensing. *Remote Sensing* 13(20): 13–26. DOI: <http://dx.doi.org/10.3390/rs13204155>
- Allen R, Morton C, Kamble B, Kilic A, Huntington J, Thau D, Gorelick N, Erickson T, Moore R, Trezza R, et al (2015) EEFlux: A landsat-based evapotranspiration mapping tool on the Google Earth Engine. *Joint ASABE/IA Irrigation Symposium 2015: Emerging Technologies for Sustainable Irrigation*: 424–433. DOI: <http://dx.doi.org/10.13031/irrig.20152143511>

- Allen R, Pereira LS, Raes D, Smith M (1998) FAO Irrigation and Drainage Paper Crop. Available: <http://www.kimberly.uidaho.edu/water/fao56/fao56.pdf>
- Allen R, Tasumi M, Morse A, Trezza R, Wright JL, Bastiaanssen W, Kramber W, Lorite I, Robison CW (2007) Satellite-Based Energy Balance for Mapping Evapotranspiration with Internalized Calibration (METRIC)-Model. *Journal of Irrigation and Drainage Engineering* 133(4): 395-406. DOI: [http://dx.doi.org/10.1061/\(asce\)0733-9437\(2007\)133:4\(395\)](http://dx.doi.org/10.1061/(asce)0733-9437(2007)133:4(395))
- Alvares CA, Stape JL, Sentelhas PC, Moraes Gonçalves JL de, Sparovek G (2013) Köppen's climate classification map for Brazil. *Meteorologische Zeitschrift* 22(6): 711–728. DOI: <http://dx.doi.org/10.1127/0941-2948/2013/0507>
- Barkhordari S, Hashemy Shahdany SM (2022) A systematic approach for estimating water losses in irrigation canals. *Water Science and Engineering* 15(2): 161–169. DOI: <http://dx.doi.org/10.1016/j.wse.2022.02.004>
- Bastiaanssen WGM, Pelgrum H, Wang J, Ma Y, Moreno JF, Roerink GJ, Van Der Wal T (1998) A remote sensing surface energy balance algorithm for land (SEBAL): 1. Formulation. *Journal of Hydrology* 212–213 (1–4): 213–229. DOI: [http://dx.doi.org/10.1016/S0022-1694\(98\)00254-6](http://dx.doi.org/10.1016/S0022-1694(98)00254-6)
- Bazzi CL, Jasse EP, Graziano Magalhães PS, Michelon GK, Souza EG de, Schenatto K, Sobjak R (2019) AgDataBox API – Integration of data and software in precision agriculture. *SoftwareX* 10: 100327. DOI: <http://dx.doi.org/10.1016/j.softx.2019.100327>
- Betzek NM, Souza EG de, Bazzi CL, Schenatto K, Gavioli A (2018) Rectification methods for optimization of management zones. *Computers and Electronics in Agriculture* 146: 1–11. DOI: <http://dx.doi.org/10.1016/j.compag.2018.01.014>
- Bezerra JRC, Azevedo PV de, Silva BB da, Dias JM (2010) Evapotranspiração e coeficiente de cultivo do algodoeiro BRS-200 Marrom, irrigado. *Revista Brasileira de Engenharia Agrícola e Ambiental* 14 (6): 625–632. DOI: <http://dx.doi.org/10.1590/s1415-43662010000600009>
- Bier VA, Souza EG (2017) Interpolation selection index for delineation of thematic maps. *Computers and Electronics in Agriculture* 136: 202–209. DOI: <http://dx.doi.org/10.1016/j.compag.2017.03.008>
- Boydell B, Mcbratney AB (2002) Identifying potential within-field management zones from cotton-yield estimates. *Precision Agriculture* 3: 9–23.
- Chao L, Zhang K, Wang J, Feng J, Zhang M (2021) A comprehensive evaluation of five evapotranspiration datasets based on ground and grace satellite observations: Implications for improvement of evapotranspiration retrieval algorithm. *Remote Sensing* 13 (12): 1–18. DOI: <http://dx.doi.org/10.3390/rs13122414>
- Chastain DR, Snider JL, Collins GD, Perry CD, Whitaker J, Byrd SA, Oosterhuis DM, Porter WM (2016) irrigation scheduling using predawn leaf water potential improves water productivity in drip-irrigated cotton. *Crop Science* 56(6): 3185–3195. DOI: <http://dx.doi.org/10.2135/CROPSCI2016.01.0009>
- Del Grosso SJ, Parton WJ, Derner JD, Chen M, Tucker CJ (2018) Simple models to predict grassland ecosystem C exchange and actual evapotranspiration using NDVI and environmental variables. *Agricultural and Forest Meteorology* 249: 1–10. DOI: <http://dx.doi.org/10.1016/j.agrformet.2017.11.007>
- Fontanet M, Scudiero E, Skaggs TH, Fernández-García D, Ferrer F, Rodrigo G, Bellvert J (2020) Dynamic management zones for irrigation scheduling. *Agricultural Water Management* 238: 106207. DOI: <http://dx.doi.org/10.1016/j.agwat.2020.106207>
- Fridgen JJ, Fraisse CW, Kitchen NR, Sudduth KA (2000) Delineation and analysis of site-specific management zones. In: *International Conference on Geospatial Information in Agriculture and Forestry. Proceedings...*
- Fridgen JJ, Kitchen NR, Sudduth KA, Drummond ST, Wiebold WJ, Fraisse CW (2004) Management zone analyst (MZA): software for subfield management zone delineation. *Agronomy Journal* 96 (1): 100.
- Gobbo S, Lo Presti S, Martello M, Panunzi L, Berti A, Morari F (2019) Integrating SEBAL with in-field crop water status measurement for precision irrigation applications-a case study. *Remote Sensing* 11 (17): 1–18. DOI: <http://dx.doi.org/10.3390/rs11172069>
- Grosso C, Manoli G, Martello M, Chemin YH, Pons DH, Teatini P, Piccoli I, Morari F (2018) Mapping maize evapotranspiration at field scale using SEBAL: A comparison with the FAO method and soil-plant model simulations. *Remote Sensing* 10(9). DOI: <http://dx.doi.org/10.3390/rs10091452>
- Kalma JD, Jupp DLB (1990) Estimating evaporation from pasture using infrared thermometry: evaluation of a one-layer resistance model. *Agricultural and Forest Meteorology* 51(3–4): 223–246. DOI: [http://dx.doi.org/10.1016/0168-1923\(90\)90110-R](http://dx.doi.org/10.1016/0168-1923(90)90110-R)
- Köppen W (1884) Die Wärmezonen der Erde, nach der Dauer der heissen, gemässigten und kalten Zeit und nach der Wirkung der Wärme auf die organische Welt betrachtet. *Meteorologische Zeitschrift*: 215–226.
- Mendes WR, Araújo FMU, Dutta R, Heeren DM (2019) Fuzzy control system for variable rate irrigation using remote sensing. *Expert Systems with Applications* 124: 13–24. DOI: <http://dx.doi.org/10.1016/j.eswa.2019.01.043>
- Menenti M, Choudhury BJ (1993) Parameterization of land surface evaporation by means of location dependent potential evaporation and surface temperature range. In *Proceedings of the Yokohama Symposium IAHS Publ*; 561–568.

- Michelon GK, Bazzi CL, Upadhyaya S, de Souza EG, Magalhães PSG, Borges LF, Schenatto K, Sobjak R, Gavioli A, Betzek NM (2019) Software AgDataBox-Map to precision agriculture management. *SoftwareX* 10: 100320. DOI: <http://dx.doi.org/10.1016/j.softx.2019.100320>
- Morais R, Silva N, Mendes J, Adão T, Pádua L, López-Riquelme JA, Pavón-Pulido N, Sousa JJ, Peres E (2019) mySense: A comprehensive data management environment to improve precision agriculture practices. *Computers and Electronics in Agriculture* 162: 882–894. DOI: <http://dx.doi.org/10.1016/j.compag.2019.05.028>
- Neupane J, Guo W (2019) Agronomic basis and strategies for precision water management: A review. *Agronomy* 9 (2): 1–21. DOI: <http://dx.doi.org/10.3390/agronomy9020087>
- Pershing T, County O, Missouri T, Railway T, Cochahee N, Cochahee S, Bulletin GS, Agency OI (2012) Progress report on a subsurface study of the pershing oil and gas field, Osage County, (P Steduto, TC Hsiao, E Fereres, and D Raes, eds). *FAO IRRIGATION AND DRAINAGE PAPER*: Rome.
- Peschechera G, Lamaddalena N, Fratino U (2019) Estimation of irrigation water requirements at irrigation district level using MODIS evapotranspiration product. In *Seventh International Conference on Remote Sensing and Geoinformation of the Environment (RSCy2019) SPIE*: 146–155. DOI: <http://dx.doi.org/10.1117/12.2533475>
- Pimentel-Gomes F (2009) Curso de estatística experimental (FEALQ, ed.). Piracicaba - SP. Available: <http://fealq.org.br/produto/curso-de-estatistica-experimental-15a-edicao/>. Accessed Nov 17, 2018.
- Ping JL, Dobermann A (2003) Creating spatially contiguous yield classes for site-specific management. *Agronomy Journal* 95 (5): 1121–1131. DOI: <http://dx.doi.org/10.2134/agronj2003.1121>
- Pokorny J (2019) Evapotranspiration. *Encyclopedia of Ecology* 2: 292–303. DOI: <http://dx.doi.org/10.1016/B978-0-12-409548-9.11182-0>
- QGIS Development Team (2021) QGIS Geographic Information System Available: <https://www.qgis.org>. Accessed Apr 8, 2021.
- Rosolem CA (2001) *Ecofisiologia e manejo da cultura do algodoeiro*. Botucatu.
- Rousseeuw PJ (1987) Silhouettes: a graphical aid to the interpretation and validation of cluster analysis Available: [https://ac.els-cdn.com/0377042787901257/1-s2.0-0377042787901257-main.pdf?\\_tid=6e43cc3c-f9b5-4088-b40e-a1717784b9db&acdnat=1541967792\\_30449939409e63aff364db54892725e2](https://ac.els-cdn.com/0377042787901257/1-s2.0-0377042787901257-main.pdf?_tid=6e43cc3c-f9b5-4088-b40e-a1717784b9db&acdnat=1541967792_30449939409e63aff364db54892725e2). Accessed Nov 11, 2018.
- Rozenstein O, Haymann N, Kaplan G, Tanny J (2019) Validation of the cotton crop coefficient estimation model based on Sentinel-2 imagery and eddy covariance measurements. *Agricultural Water Management* 223: 105715. DOI: <http://dx.doi.org/10.1016/j.agwat.2019.105715>
- Schenatto K, Souza EG de, Bazzi CL, Gavioli A, Betzek NM, Beneduzzi HM (2017) Normalization of data for delineating management zones. *Computers and Electronics in Agriculture* 143: 238–248. DOI: <https://doi.org/10.1016/j.compag.2017.10.017>
- Sharma V, Irmak S (2021) Comparative analyses of variable and fixed rate irrigation and nitrogen management for maize in different soil types: Part I. Impact on soil-water dynamics and crop evapotranspiration. *Agricultural Water Management* 245: 106644. DOI: <https://doi.org/10.1016/j.agwat.2020.106644>
- Shen Q, Wang Y, Wang X, Liu X, Zhang X, Zhang S (2019) Comparing interpolation methods to predict soil total phosphorus in the Mollisol area of Northeast China. *Catena* 174: 59–72. DOI: <http://dx.doi.org/10.1016/j.catena.2018.10.052>
- Souza V de A, Roberti DR, Ruhoff AL, Zimmer T, Adamatti DS, de Gonçalves LGG, Diaz MB, Alves R de CM, de Moraes OL (2019) Evaluation of MOD16 algorithm over irrigated rice paddy using flux tower measurements in Southern Brazil. *Water* 11(9). DOI: <http://dx.doi.org/10.3390/w11091911>
- Teixeira AH de C (2010) Determining Regional Actual Evapotranspiration of Irrigated Crops and Natural Vegetation in the São Francisco River Basin (Brazil) Using Remote Sensing and Penman-Monteith Equation. *Remote Sensing* 2(5): 1287–1319. DOI: <http://dx.doi.org/10.3390/rs0251287>
- Venancio LP, Mantovani EC, Do Amaral CH, Neale CMU, Filgueiras R, Gonçalves IZ, da Cunha FF (2020) Evapotranspiration mapping of commercial corn fields in Brazil using safer algorithm. *Scientia Agricola* 78(4): 1–12. DOI: <http://dx.doi.org/10.1590/1678-992x-2019-0261>
- Yang L, Li J, Sun Z, Liu J, Yang Y, Li T (2022) Daily actual evapotranspiration estimation of different land use types based on SEBAL model in the agro-pastoral ecotone of northwest China. *PLoS ONE* 17 (3): e0265138. DOI: <http://dx.doi.org/10.1371/JOURNAL.PONE.0265138>
- Yao RJ, Yang JS, Zhang TJ, Gao P, Wang XP, Hong LZ, Wang MW (2014) Determination of site-specific management zones using soil physico-chemical properties and crop yields in coastal reclaimed farmland. *Geoderma* 232–234: 381–393. DOI: <https://doi.org/10.1016/j.geoderma.2014.06.006>